Published in final edited form as:
*J Neurophysiol*. 2007 September ; 98(3): 1181–1193. doi:10.1152/jn.00370.2007.

# Emergence of Multiplicative Auditory Responses in the Midbrain of the Barn Owl

**Brian J. Fischer**[1], **José Luis Peña**[2], and **Masakazu Konishi**[1]

1*Division of Biology, California Institute of Technology, Pasadena, California*

2*Department of Neuroscience, Albert Einstein College of Medicine, Bronx, New York*

## Abstract

Space-specific neurons in the barn owl's auditory space map gain spatial selectivity through tuning to combinations of the interaural time difference (ITD) and interaural level difference (ILD). The combination of ITD and ILD in the subthreshold responses of space-specific neurons in the external nucleus of the inferior colliculus (ICx) is well described by a multiplication of ITD- and ILD-dependent components. It is unknown, however, how ITD and ILD are combined at the site of ITD and ILD convergence in the lateral shell of the central nucleus of the inferior colliculus (ICcl) and therefore whether ICx is the first site in the auditory pathway where multiplicative tuning to ITD- and ILD-dependent signals occurs. We used extracellular re-cording of single neurons to determine how ITD and ILD are combined in ICcl of the anesthetized barn owl (*Tyto alba*). A comparison of additive, multiplicative, and linear-threshold models of neural responses shows that ITD and ILD are combined nonlinearly in ICcl, but the interaction of ITD and ILD is not uniformly multiplicative over the sample. A subset (61%) of the neural responses is well described by the multiplicative model, indicating that ICcl is the first site where multiplicative tuning to ITD- and ILD-dependent signals occurs. ICx, however, is the first site where multiplicative tuning is observed consistently. A network model shows that a linear combination of ICcl responses to ITD–ILD pairs is sufficient to produce the multiplicative subthreshold responses to ITD and ILD seen in ICx.

## INTRODUCTION

A critical component of information processing in neural systems is the performance of nonlinear operations on sensory variables. Multiplication is a basic nonlinear operation that is suggested to play a role in many aspects of neural computation (Koch 1999; Koch and Poggio 1992; Mel 1990; Pouget and Sejnowski 1997; Salinas and Abbott 1997; Stern and Colburn 1978), but there are few model systems where multiplication can be studied (Andersen et al. 1997; Egelhaaf et al. 1989; Gabbiani et al. 2002; Sun and Frost 1998). Here, we examine the processing of sound localization cues in the barn owl's auditory system, where multiplication is believed to contribute to the generation of the owl's auditory space map (Peña and Konishi 2001).

Space-specific neurons in the barn owl's auditory space map gain spatial selectivity as a result of tuning to combinations of the interaural time difference (ITD) and interaural level difference (ILD) (Moiseff and Konishi 1981; Olsen et al. 1989). The localization cues ITD and ILD are processed in parallel path-ways in the brain stem (Moiseff and Konishi 1983; Sullivan and Konishi 1984; Takahashi et al. 1984) that converge in the lateral shell of the central nucleus

Address for reprint requests and other correspondence: B. J. Fischer, California Institute of Technology, Division of Biology, Mail code 216-76, 1200 E. California, Pasadena, CA 91125 (E-mail: fischerb@caltech.edu).

of the inferior colliculus (ICcl) (Takahashi and Konishi 1988; Takahashi et al. 1988). Outputs from ICcl convey ITD and ILD to the external nucleus of the inferior colliculus (ICx) where the auditory space map is generated (Knudsen 1983; Knudsen and Konishi 1978a). The combination of ITD and ILD in the subthreshold responses of space-specific neurons in ICx is well described by a multiplication of an ITD-dependent component and an ILD-dependent component (Peña and Konishi 2001). It is unknown, however, how ITD and ILD are combined in ICcl and therefore whether ICx is the first site in the auditory pathway where multiplicative tuning to ITD- and ILD-dependent signals occurs.

We used extracellular recording of single neurons to determine how ITD and ILD are combined in ICcl. By comparing additive, multiplicative, and linear-threshold models of neural responses, we show that ITD and ILD are combined nonlinearly in ICcl, but the interaction of ITD and ILD is not uniformly multiplicative over the sample. A subset of the neural responses is well described by a multiplicative interaction of ITD- and ILD-dependent components, indicating that ICcl is the first site where multiplicative responses occur. A network model is used to show that a weighted sum of ICcl responses is sufficient to produce the multiplicative responses seen in ICx.

## METHODS

Extracellular recordings of isolated neurons were made in four anesthetized adult barn owls (*Tyto alba*). Experimental procedures followed the National Institutes of Health *Guide for the Care and Use of Laboratory Animals* and were approved by the Institutional Animal Care and Use Committee of the California Institute of Technology.

### Surgery

Owls were anesthetized with intramuscular injections of ketamine (20 mg/kg; Ketaject; Phoenix Pharmaceuticals, St. Joseph, MO) and xylazine (2 mg/kg; Xyla-Ject; Phoenix Pharmaceuticals). Owls were also given an intramuscular injection of antibiotics (oxytetracycline, 20 mg; maxim-200; Phoenix Pharmaceuticals) and a subcutaneous injection of lactated ringer's solution (B. Braun Medical, Irvine, CA) at the beginning of each session. Subsequent injections of ketamine and xylazine were given as needed to maintain an adequate level of anesthesia (approximately every 2 h). The owl was restrained with a soft leather jacket and covered with a water-based heating pad (k-20-f; American Medical Systems, Cincinnati, OH) to maintain the body temperature. In the initial experiment, a head plate and zero post were fixed to the owl's skull to facilitate stereotaxic localization of the recording area (Arthur 2004). A craniotomy was made to expose the area between 4 and 5 mm lateral to the zero post. At each recording session, the dura was incised and reflected with a hypodermic needle and an electrode was lowered to the desired depth. At the end of the recording session, the opening in the skull was filled with dental cement and the wound was sutured. The owl remained isolated in a heated cage overnight.

### Acoustic stimuli

Custom software was used to generate sound stimuli (Arthur 2004). Stimuli consisted of broadband noise and tones 100 ms in duration with 5-ms linear rise and fall ramps. Broadband noise stimuli had a passband of 0.5–12 kHz. Stimulus ITD was varied in steps of 30 μs, ILD in steps of 3–5 dB, average binaural level (ABL) in steps of 5 dB, and frequency in steps of 500 Hz.

All recordings took place in a double-walled sound-attenuating chamber (Industrial Acoustics, Bronx, NY). Acoustic stimuli were delivered by a stereo analog interface [DD1; Tucker Davis Technologies (TDT), Gainesville, FL] through a calibrated earphone assembly. Each earphone

consisted of a transducer (Knowles 1914; Knowles, Itasca, IL) and a microphone (Knowles 1319) encased in a custom-made metal delivery piece that fits in the owl's ear canal. Gaps between the earphone assembly and the ear canal were filled with silicon impression material (gold Velvet II; All American Mold Laboratories, Oklahoma City, OK). The microphone was used to measure the transducer's frequency response. The inverse of the transducer's frequency response was then applied to outgoing stimuli (Arthur 2004).

## Data collection

Extracellular recordings of single ICcl neurons were made with tungsten electrodes (1 MΩ, 0.005-in.; A–M Systems, Carlsborg, WA). The mediolateral and anteroposterior positions of the electrode were set with a custom-made micromanipulator (Narishige, Tokyo, Japan) using known stereotaxic coordinates. Electrodes were advanced coarsely in the dorsoventral dimension using the micromanipulator until the electrode tip was about 1 mm from the dorsal border of ICcl. Fine dorsoventral movements were made with a remote-controlled microdrive (Motion Controller, Model PMC 100; Newport, Irvine, CA). Neurons were considered isolated based on the presence of a refractory period in the interspike interval histogram and the similarity of spike shape.

Action potentials were amplified, filtered (Amplifier System, μA-200; Beckman Electronic Shop, Pasadena, CA), and converted to transistor–transistor logic pulses with a spike discriminator (SD1; TDT). Data were stored in a computer by a time converter (ET1; TDT) and an A/D converter (DD1; TDT) with a sampling rate of 48 kHz and 16-bit resolution.

The data for this study consist of spike counts in response to sound stimuli with fixed ITD, ILD, ABL, and, for tones, frequency. The following protocol was used once a neuron was isolated. The best ITD and ILD of the neuron were determined by varying the ITD and ILD of a broadband noise stimulus. The threshold of the neuron was then determined using a broadband noise stimulus at the best ITD and ILD. The threshold was defined as the smallest ABL where the neuron had a spike count that exceeded the spontaneous spike count. The spike count response to a matrix of ITD and ILD values of a broadband noise stimulus was collected at a stimulus level that was 15–20 dB above threshold. If possible, the response of the neuron to the ABL of a noise stimulus at the best ITD and ILD was measured for a larger range of ABL than was used in the threshold calculation. This is called the rate-level function. Also, the response to the frequency of a tonal stimulus at a fixed stimulus intensity was collected at the best ITD and ILD at a stimulus level that was 15–20 dB above threshold. This is called the isointensity frequency tuning curve. For rate-level functions, ITD–ILD matrices, and isointensity frequency tuning curves, stimulus parameters were varied randomly. Spike counts were averaged over three to ten repetitions for each parameter value. At least five repetitions were used in 70 of 77 neurons.

We used known stereotaxic coordinates to position the electrode for recording from ICcl, which was then distinguished from ICx based on tuning to ILD and frequency at multiple sites during each penetration (Brainard and Knudsen 1993). In ICx, best ILDs progress from right-ear greater, corresponding to directions above the horizontal plane, to left-ear greater, corresponding to directions below the horizontal plane, with depth (Knudsen and Konishi 1978b). Also, neurons in ICx have broad tuning to stimulus frequency and best frequency is not mapped (Knudsen and Konishi 1978b). In ICcl, most units are narrowly tuned to frequency, best frequency increases with depth, and best ILD does not vary systematically with depth (Knudsen and Konishi 1978b; Wagner et al. 1987). During each penetration, several multiunit recordings were made to examine the progression of best ITD, best ILD, and best frequency with depth. Units were considered to belong to ICcl if the progression of responses followed the previously documented pattern. In addition to using the progression of responses as a guide,

we limited our analysis to neurons with frequency tuning curve widths that were <2.5 kHz, in accordance with previous studies (Brainard and Knudsen 1993).

## Histology

Recording sites were marked in two owls using electrolytic lesions. Lesions were made by passing −3-μA DC for 10 s one to three times. A week after the lesions were made, the owls were overdosed with sodium pentobarbital (Nembutal; Abbott Laboratories, North Chicago, IL) and perfused with saline, followed by 2% paraformaldehyde (Fisher Scientific, Fair Lawn, NJ). Brains were blocked in the plane of the electrode penetration, removed from the skull, and placed in 30% sucrose until they sank. They were then cut in 40-μm sections and mounted on slides to verify the location of the recording site.

## Data analysis

**FREQUENCY TUNING—**The best frequency is the frequency that elicits the maximum spike count in the isointensity frequency tuning curve. The half-height width is the width of the peak in the tuning curve at half the distance between the minimum and maximum responses.

**THRESHOLDS—**In the off-line analysis reported in the results, the neural threshold is the smallest ABL where the rate-level function has a response that is significantly greater than the spontaneous response at that value and for all greater values of ABL. A *t*-test at the 5% level was used to determine that a response was significantly greater than the spontaneous response. The spontaneous response is the average spike count in an interval of 100 ms before stimulus onset.

**ITD AND ILD TUNING—**ITD and ILD tuning were assessed using properties of ITD and ILD tuning curves derived from the ITD–ILD response matrix. The ITD–ILD response matrix is a matrix containing the average spike count responses to ITD–ILD pairs, where ITD and ILD vary along rows and columns, respectively. The best ITD and ILD are the parameter values that elicit the largest response. The ITD tuning curve is the mean spike count as a function of ITD at the best ILD of the neuron and vice versa.

ITD tuning curves of neurons with narrow frequency tuning often display multiple peaks (Wagner et al. 1987). The relative spike count produced at the main peak and side peaks of ITD tuning curves was quantified using the side peak suppression (SPS), where SPS = [(MP – SP)/MP] × 100%. Here, MP is the spike count produced at the main peak and SP is the spike count produced at the largest side peak.

The trough:peak ratio for an ITD tuning curve is the ratio of the spike count at the trough of the curve to the spike count at the peak of the curve. The peak and trough of the curve are the ITD values where the maximum and minimum spike counts are observed, respectively.

The half-height width of a tuning curve for ITD or ILD is the width of the peak in the tuning curve at half the distance between the minimum and maximum responses. If one flank of the tuning curve remains above the half-maximum height over the range of ITD or ILD values used, then the tuning curve half-peak width is undefined.

Symmetry of ILD tuning curves was quantified by comparing the area under the tuning curve on both sides of the peak. The difference in area is given by the symmetry index $\sum_n [R(i-n) - R(i+n)]^2$, where $R$ is the ILD tuning curve normalized by the difference between the maximum and minimum points, the peak occurs at the $i$th ILD value, and the sum is taken over an equal number of points greater and smaller than the peak value (Peña and Konishi 2002).

ILD tuning curves of ICcl neurons have previously been classified as one of sigmoidal, open-peaked, or peaked (Mazer 1995). The multiplicative model of ITD–ILD interaction implies that ILD tuning curves at different ITDs should be modulated versions of each other, but that the shape should not change with ITD. We quantified the shape of ILD tuning curves at different ITD values using a measure that is invariant under changes in ITD if the multiplicative model of ITD–ILD interaction holds. For each ITD, the ILD tuning curve shape was quantified by the height of the ILD tuning curve flank with the largest response, divided by the maximum spike count over all ILD values. The height of the largest ILD tuning curve flank is the maximum of the spike counts produced at the endpoints of the ILD range, denoted $R_h$. Therefore the flank-height is given by $[R_h/\max(R)] \times 100\%$. A tuning curve flank-height of 100% corresponds to a sigmoidal curve, whereas lower values correspond to open-peaked or peaked curves by previous classifications (Mazer 1995).

The change in the best ITD with ILD was quantified as the slope of the minimum mean square linear fit of best ITD as a function of ILD for neurons where there were at least five significant ITD tuning curves and the root-mean-square (RMS) error in the best linear fit was ≤30 μs. An ITD tuning curve is considered significant if the spike count at the peak is significantly different from zero as determined by a Wilcoxon signed-rank test for zero median and the spike count at the peak is ≥25% of the maximum spike count produced at any ITD–ILD pair. This is a conservative measure of significance that ensures that overestimates are not made of the variability of best ITD with ILD. The same procedure was used to quantify the change in best ILD with ITD for neurons where there were at least five significant ILD tuning curves and the RMS error in the best linear fit was ≤6 dB.

**MODELS OF RESPONSES TO ITD AND ILD—**Spiking responses of ICcl neurons to ITD and ILD were fit with an additive model, a multiplicative model, and a linear-threshold model.

In the additive model, the matrix of spike count responses to pairs of stimulus ITD and ILD, denoted $R$, is approximated as the minimum mean square model of the form

$$\widehat{R}(j,k) = R_a + G(j) + H(k)$$

where $G(\cdot)$ is a function of ITD, $H(\cdot)$ is a function of ILD, and $R_a$ is a constant (Peña and Konishi 2001).

The multiplicative model is specified in terms of the singular value decomposition (SVD) of the response matrix after the subtraction of a constant bias (Peña and Konishi 2001). A multiplicative model of the response matrix is obtained using the first singular vectors $U_1$ and $V_1$ weighted by the first singular value $\sigma_1$ added to a constant bias $R_m$, yielding

$$\widehat{R} = R_m + \sigma_1 U_1 V_1^T$$

The constant $R_m$ is the value between the minimum and maximum spike count that minimizes the mean square error in the model fit to the data.

The fractional energy in the first singular value of the SVD was used as a measure of the ability of the multiplicative model to capture the neuron's response to ITD and ILD (Peña and Konishi 2001). With the SVD of the response matrix minus a constant expressed as $R - R_m = \sum_n \sigma_n U_n V_n^T$ the fractional energy in the first singular value is given by

$$\text{Fractional energy} = \frac{\sigma_1^2}{\sum_n \sigma_n^2} \times 100\%$$

The significance of the singular values was evaluated using a perturbation method. A confidence interval for each singular value was obtained through the following algorithm. For $N = 10$ trials, each entry of the response matrix minus a constant was corrupted with additive noise drawn from a Gaussian distribution having zero mean and a SD equal to the largest sample SD of spike counts observed for all ITD and ILD values. The resulting matrix $R - R_m + \varepsilon$, where $\varepsilon$ is a matrix of noise values, was fit as a linear combination of the matrices $U_n V_n^T$. The confidence interval for the *i*th singular value was $\mu_i \pm t_{\alpha/2}(N-1)s_i/\sqrt{N}$, where $\mu i$ and $s_i$ are the sample average and SD, respectively, of the coefficient of $U_i V_i^T$, $t_{\alpha/2}(N-1)$ is the value such that $P[T \geq t_{\alpha/2}(N-1)] = \alpha/2$, where $T$ has a Student's $t$ distribution with $(N-1)$ degrees of freedom, and $\alpha = 0.001$. The *i*th singular value is considered significant if the confidence interval does not contain zero.

In the linear-threshold model, the matrix of spike count responses to pairs of stimulus ITD and ILD is approximated as the minimum mean square model of the form

$$\widehat{R}(j,k) = R_{th} + [G(j) + H(k) - R_{th}]_+$$

where $G(\cdot)$ is a function of ITD, $H(\cdot)$ is a function of ILD, $R_{th}$ is a constant, and $[\cdot]_+$ signifies rectification.

Errors in the model approximations to the data are expressed as RMS errors that are normalized by the difference between the maximum and minimum values of the response matrix. This quantity is referred to as the normalized root-mean-square error (nRMSE).

**Modeling ICx subthreshold responses—**A model of the generation of ICx subthreshold responses from ICcl spiking responses was developed using the spike count data presented here and the subthreshold responses of ICx neurons presented in Peña and Konishi (2001). We built the model to see whether ICx subthreshold responses could be produced from a linear combination of ICcl spiking responses.

For each ICx neuron, we modified the set of ITD–ILD responses of ICcl neurons to create a realistic set of inputs to the given ICx neuron. In integrating inputs from ICcl, there is a topographic projection of ITD-sensitive neurons such that an ICx neuron will receive inputs from ICcl neurons that have similar preferred ITDs to its own (Wagner et al. 1987). Also, although ICx neurons have broader frequency tuning curves than those seen in ICcl, frequency tuning curves from ICx neurons suggest that the integration of information over frequency channels is restricted (Mazer 1995; Mori 1997). In this study, ICcl neurons were recorded from multiple locations in the nucleus. These neurons had a wide range of best frequencies and best ITDs. To create a suitable set of ICcl inputs to a given ICx neuron, each ICcl neuron's response was transformed by altering the best ITD and best frequency in a parametric fit to the ICcl neuron's response (Fig. 10). Each column of the ITD–ILD response matrix, where ITD varies and ILD is fixed, was fit by a function of the form

$$R(j,k) = a_k + b_k \exp\left\{c_k \cos[2\pi f_k(\mathrm{ITD}_j - \mu_k)] - [(\mathrm{ITD}_j - \mu_k)/\sigma_k]^2\right\}$$

where the parameters $a_k$, $b_k$, $c_k$, $f_k$, $\mu_k$, and $\sigma_k$, were determined for each ILD. The exponentiated cosine term creates a cyclic variation in ITD and the Gaussian term produces side peak suppression. The parametric fit to the response of each neuron was transformed by replacing the frequency $f_k$, and the center ITD $\mu_k$ of the ITD tuning curves.

For each ICx neuron, we computed the best ITD $\mu_d$ and best frequency $f_d$. The best ITD and best frequency of the ICcl inputs were then drawn from Gaussian distributions centered at the best ITD and best frequency of the ICx neuron. The SD of the best ITD distribution was 5 μs and the SD of the best frequency distribution was 1 kHz. (Note that this does not imply that

the ICx units have Gaussian-shaped frequency tuning curves.) The parametric fit of each ICcl neuron was modified so that the pattern of variation of its best ITD with ILD would remain, but the best ITD and frequency of the main ITD tuning curve would match the desired value. This was accomplished by making the substitutions $\mu_k \rightarrow \mu_k - \mu_{best} + \mu_d$ and $f_k \rightarrow f_k - f_{best} + f_d$, where $\mu_{best}$ and $f_{best}$ are the original parameter values for the ICcl neuron's ITD curve at the best ILD.

The subthreshold response of the ICx neuron, denoted $V_{ICx}$, was approximated as a linear combination of the shifted versions of the spike count responses of the ICcl neurons

$$\widehat{V}_{ICx}(j,k) = V_o + \sum_{i=1}^{N} \omega_i R_{ICcl,i}(j,k)$$

where $V_o$ is a constant and $R_{ICcl,i}$ is the parametric fit of the $i$th ICcl neuron's spike count response with a shifted best ITD and best frequency. The ICcl units in the model are referred to as hidden units to differentiate between the shifted responses used in the model and the measured responses. The connection weights were found by minimizing a cost function consisting of a mean square approximation error plus a regularization term given by

$$E = \sum_{j=1}^{N_{\mathrm{ITD}}} \sum_{k=1}^{N_{\mathrm{ILD}}} [V_{ICx}(j,k) - V_o - \sum_{i=1}^{N} \omega_i R_{ICcl,i}(j,k)]^2 + 0.1 \sum_{i=1}^{N} \omega_i^2$$

The regularization term causes the weight density to be distributed more uniformly over the ICcl population. The range of ITD values for the ICx subthreshold responses was limited to ±210 μs and the range of ILD values was limited to ±20 dB.

## RESULTS

Spike count responses to ITD and ILD were collected from 77 isolated ICcl neurons in four barn owls. We observed a diversity of responses to ITD and ILD in ICcl (Fig. 1). Many neurons responded only when both ITD and ILD were within particular ranges (Fig. 1, *A* and *B*, Fig. 2, Fig. 9*A*, and Fig. 10). This response type is indicative of an AND gate and is what gives space-specific neurons their selectivity. Most neurons had phase-ambiguous responses to stimulus ITD as a result of narrow tuning to stimulus frequency and therefore displayed multiple regions of similar responses as ITD varied (Fig. 1, *A*, *B*, and *F*, Fig. 2, Fig. 9*A*, and Fig. 10). Several neurons were tuned to both ITD and ILD, but showed limited ITD tuning at one end of the ILD range even though the neuron responded to the sound (Fig. 1, *C* and *D* and Fig. 3). A small number of neurons had clear tuning to either ITD or ILD, but had limited response modulation to the other variable (Fig. 1, *E* and *F*).

We examined the responses to ITD and ILD to see whether the interaction between ITD and ILD is consistent with a multiplicative model.

### Models of responses to ITD and ILD

We compared three models of ITD–ILD interaction in the spiking responses of the recorded neurons. Spiking responses to ITD and ILD were fit with models given by additive or multiplicative interaction of ITD- and ILD-dependent components, following the analysis of ICx responses by Peña and Konishi (2001). We considered the possibility that thresholding, not multiplication, describes the AND gate–type of selectivity for ITD and ILD seen in the sample. Therefore spiking responses were also fit with a linear-threshold model given by additive interaction of ITD- and ILD-dependent components followed by a rectifying nonlinearity (see METHODS for model details).

**MODEL ACCURACY—**The multiplicative model of ITD–ILD interaction better fit the data than did the additive model in most (73/77) neurons (Fig. 4). The mean normalized RMS error (see METHODS for definition) was 3.87% larger for the additive model than for the multiplicative model (11.00 ± 2.21 vs. 7.13 ± 2.81%; mean ± SD; paired *t*-test; $P < 0.0001$). As seen in Fig. 2, the multiplicative model captured the characteristic feature of most responses, the limitation of spiking to discrete regions of ITD and ILD. The additive model was unable to produce this type of response. However, the additive model did provide a better fit than the multiplicative model in four neurons (see, e.g., Fig. 3). The largest improvement in the normalized RMS error for the additive model over the multiplicative model was 1.78%.

The linear-threshold model of ITD–ILD interaction better fit the data than did the additive model in all neurons (Fig. 4). The mean nRMSE was 3.32% larger for the additive model than for the linear-threshold model (11.00 ± 2.21 vs. 7.68 ± 2.78%; paired *t*-test; $P < 0.0001$). As seen in Fig. 2, the linear-threshold model produced the AND gate selectivity that was reproduced in the multiplicative model, but was absent in the additive model.

The multiplicative model of ITD–ILD interaction better fit the data than did the linear-threshold model in a majority (57/77) of neurons (Fig. 4). The mean nRMSE was 0.55% larger for the linear-threshold model than for the multiplicative model (7.68 ± 2.78 vs. 7.13 ± 2.81%; paired *t*-test; $P < 0.0001$). Although both the multiplicative and linear-threshold models produced AND gate responses, only the multiplicative model displayed the smooth transitions between regions of zero response and regions of positive response that were commonly observed in the data (Fig. 2).

**CONTRIBUTION OF MULTIPLICATION TO THE OBSERVED NONLINEARITY—**We evaluated the accuracy of the multiplicative model using the distribution of energy over the singular values in the singular value decomposition of each ITD–ILD response matrix. For a purely multiplicative response, all of the energy is concentrated in the first singular value. After subtracting away a constant from the ITD–ILD response matrix, the mean fractional energy in the first singular value was 90.37 ± 7.21% (median 92.67%, first quartile 86.44%, third quartile 96.03%) (Fig. 5). A majority of the neurons (47/77) had a fractional energy in the first singular value that was ≥91.15% and therefore fell into the range observed for the subthreshold responses of ICx neurons by Peña and Konishi (2001).

For a majority of neurons, the multiplicative model did not completely describe the interaction of ITD and ILD in generating the response. The fractional energy in the second singular value had a mean of 5.11 ± 4.52% and was as large as 23.97%. We used a perturbation method (see METHODS) to test the significance of the second singular value. For a 99.9% confidence interval with 9 df (degrees of freedom), 48/77 neurons had a significant second singular value.

### Correlations between multiplicative tuning and general response properties

The degree to which neurons showed multiplicative tuning to ITD- and ILD-dependent components was very weakly correlated with other response properties. We considered two measures of the degree to which neurons showed multiplicative tuning, the energy in the first singular value and the difference in the nRMSE between the additive and multiplicative models. The response properties examined included those that describe what stimulus parameters are preferred by the neurons (best frequency, best ITD, and best ILD) and those that are associated with the degree of spatial selectivity of a neuron (ITD tuning curve width, side peak suppression, ILD tuning curve width, ILD tuning curve symmetry, threshold, and frequency tuning curve width). For both measures of multiplicative tuning, the squared correlation coefficient $r^2$ was ≤0.13 for all response properties considered.

## Consistency with and deviations from multiplication

Although the fit to the data were better for the multiplicative model than for the additive model for most cells, there were properties of the neural responses to ITD and ILD that are not consistent with multiplication. The multiplicative model of ITD–ILD interaction implies that an ITD tuning curve at one ILD should be a modulated version of the ITD tuning curve at any other ILD. Similarly, an ILD tuning curve at one ITD should be a modulated version of the ILD tuning curve at any other ITD. One consequence of this relationship between tuning curves is that the best ITD should be independent of ILD and vice versa. Also, the shape of the tuning curves should remain constant as the other variable changes. This means that the trough:peak ratio for ITD tuning curves should be independent of ILD and the height of the largest ILD tuning curve flank should be independent of ITD.

Many neurons qualitatively agreed with the multiplicative model and had similar tuning curves for each value of the other variable (see, e.g., Fig. 6, *A–C*). There were also neurons that showed nonmultiplicative changes in ITD or ILD tuning with changes in the other variable (see, e.g., Fig. 6, *D–F*). We thus examined changes in preferred values of tuning curves and the shape of tuning curves with changes in the other variable.

**CHANGES IN ITD TUNING WITH ILD—**ITD tuning curves of some neurons shifted with changes in ILD. Systematic shifts in ITD tuning with ILD were observed that are similar to shifts of ITD tuning curves of coincidence detector neurons in nucleus laminaris (NL) (Viete et al. 1997) (Fig. 1*F* and Fig. 10). We quantified the change in best ITD with ILD by the slope of the least-squares linear fit of best ITD as a function of ILD. The rate of change was computed for neurons where ITD tuning curves were significant for at least five ILD values and the RMS error in the best linear fit was ≤30 μs (33/77; see METHODS). Both positive and negative rates of change of best ITD with ILD were observed (Fig. 7*A*). The average absolute value of the rate of change of best ITD with ILD for 33 neurons was 0.73 ± 0.63 μs/dB. The absolute value of the rate of change of best ITD with ILD was weakly correlated with the fractional energy in the first singular value of the singular value decomposition of the ITD–ILD response matrix ($r^2 = 0.19$, $P < 0.02$). However, the absolute value of the rate of change of best ITD with ILD was not correlated with the difference in the nRMSE between the additive and multiplicative models ($r^2 = 0.03$, $P > 0.3$).

In several neurons, ITD tuning disappeared at large positive or negative ILD values. For example, the neurons shown in Fig. 1, *C* and *D* had clear ITD tuning for values of ILD near zero. However, at one extreme of the ILD range the modulation of the response with ITD disappeared while the neuron still responded to the sound. Changes in the shape of ITD tuning curves across ILD were assessed by computing the trough:peak ratio for each ITD tuning curve in neurons with at least five significant ITD tuning curves (37/77). A quadratic function adequately described the variation of the trough:peak ratio as a function of ILD, indicating that the change in trough:peak ratio with ILD was systematic (Fig. 8). Examples occurred where there was little change in the trough:peak ratio with ILD (Fig. 8*A*). In other neurons, the trough:peak ratio increased at one end of the ILD range (Fig. 8*B*) or at both ends of the ILD range (Fig. 8*C*). The difference between the maximum and minimum trough:peak ratios for ITD tuning curves at different ILDs in individual neurons fell between 0 and 0.90 with a mean of 0.36 ± 0.23 (Fig. 8*D*). The multiplicative model predicts that the difference between the maximum and minimum trough: peak ratios is zero. The difference between the maximum and minimum trough:peak ratios for ITD tuning curves at different ILDs was weakly correlated with the degree of multiplicative tuning displayed by the neuron (Fig. 8, *E* and *F*).

**CHANGES IN ILD TUNING WITH ITD—**ILD tuning curves of some neurons shifted with changes in ITD. The variation in best ILD with ITD was quantified by the slope of the least-

squares linear fit of best ILD as a function of ITD. The rate of change was computed for 33 neurons where ILD tuning curves were significant for at least five ITD values and the RMS error in the best linear fit was ≤6 dB. The average absolute value of the rate of change of the best ILD with ITD for these neurons was 0.06 ± 0.09 dB/μs (Fig. 7*B*). The absolute value of the rate of change of best ILD with ITD was correlated with the fractional energy in the first singular value of the singular value decomposition of the ITD–ILD response matrix ($r^2 = 0.49$, $P < 0.0001$). However, the absolute value of the rate of change of best ILD with ITD was not correlated with the difference in the nRMSE between the additive and multiplicative models ($r^2 = 0.01$, $P > 0.5$).

Most neurons showed changes in the shape of the ILD tuning curve for different ITDs. As seen in Fig. 6*F*, ILD tuning curves may be peaked at a subset of ITD values and sigmoidal at others. We examined changes in ILD tuning curve shape for 47 neurons that had at least five significant ILD tuning curves by computing the height of the largest tuning curve flank relative to the maximum spike count for each significant ILD tuning curve. A tuning curve flank-height of 100% corresponds to a sigmoidal curve, whereas lower values correspond to open-peaked or peaked curves by previous classifications (Mazer 1995). Some neurons had little change in the ILD tuning curve flank-height as a function of ITD (Fig. 9*A*). Other neurons showed large changes in the ILD tuning curve flank-height as a function of ITD (Fig. 9*B*). The difference between the maximum and minimum ILD tuning curve flank-heights at different ITDs in individual neurons fell between 0 and 97.92 with a mean of 50.82 ± 30.49 (Fig. 9*C*). The multiplicative model predicts that the ILD tuning curve flank-height should remain constant as ITD changes. The difference between the maximum and minimum ILD tuning curve flank-heights at different ITDs was weakly correlated with the degree of multiplicative tuning displayed by the neuron (Fig. 9, *D* and *E*).

### Modeling ICx subthreshold responses from ICcl spiking responses

We constructed a network model to determine whether a linear combination of the responses to ITD and ILD observed in ICcl is sufficient to produce the multiplicative subthreshold responses to ITD and ILD seen in ICx (Peña and Konishi 2001**)**. In this model, we treat ICcl as a set of hidden units that combine ITD and ILD in a diverse set of responses. Results from studies of population coding suggest that it is possible to "read out" from the ICcl responses a function of ITD and ILD that approximates a product of ITD- and ILD-dependent components (Eliasmith and Anderson 2003; Poggio 1990; Pouget et al. 2003).

We examined the subthreshold ITD–ILD response matrices of 16 ICx neurons (Peña and Konishi 2001). For each ICx neuron, we modified the set of ITD–ILD responses of ICcl neurons to create a set of inputs to the given ICx neuron that respects the known anatomical and physiological constraints on connectivity between ICcl and ICx neurons (Fig. 10; see METHODS). For each ICx subthreshold response examined, it was possible to find connection weights between the ICcl units and the ICx unit so that the squared correlation coefficient of the ICx data and the model approximation was >0.98 (Fig. 10*G*). The energy in the connection weights was not limited to ICcl neurons that showed the most multiplicative responses (Fig. 10, *H* and *I*). In each case the connection weights consisted of both positive and negative values.

## DISCUSSION

### The representation of ITD and ILD in ICcl

Previous studies have shown that neurons in ICcl are tuned to ITD and ILD (Mazer 1995), but the interaction between ITD and ILD in ICcl has not been described. Determining the nature of ITD and ILD convergence in ICcl is a first step in discovering where and how multiplicative tuning to ITD- and ILD-dependent signals arises in the barn owl's midbrain.

Our results show that multiplicative selectivity for ITD- and ILD-dependent signals arises in ICcl, but the spiking responses to ITD and ILD are not uniformly multiplicative over the ICcl population. In a majority of neurons, including those with the narrowest frequency tuning widths, a multiplicative model described the responses to ITD and ILD as well as it has in ICx. There were, however, response features that could not be captured by a multiplicative model. This created a wider distribution of combination selectivity than is observed in ICx. The wide distribution of combination selectivity observed in our sample indicates that ICcl is the first stage of the midbrain sound localization pathway where multiplication is observed, but ICx is the first site where it is observed consistently.

There was no evidence for a systematic arrangement of neurons in ICcl based on the degree of multiplicative selectivity for ITD- and ILD-dependent signals. There is a topographic representation of ITD and frequency in ICcl (Knudsen and Konishi 1978b; Wagner et al. 1987). A lack of significant correlation between multiplicative selectivity for ITD- and ILD-dependent signals and best ITD or best frequency suggests that multiplicative selectivity does not vary with the dorsoventral frequency axis or the anteroposterior ITD axis. In addition, neurons with multiplicative responses were not limited to those that prefer ITD and ILD values near zero. The combination selectivity for ITD and ILD appears diverse over the ICcl population.

## Generating ICcl responses

The responses observed in ICcl suggest that a nonlinear operation underlies the convergence of ITD and ILD, but are consistent with either a multiplicative or a linear-threshold mechanism. Previously, ICcl has been viewed as an AND gate for combining ITD and ILD in both qualitative and quantitative models (Euston 2000; Mazer 1995; Spence et al. 1989). The failure of the additive model to describe fundamental aspects of the neural responses shows that a nonlinearity must be present to describe ITD–ILD convergence in ICcl. This is consistent with the AND gate model, but a pure multiplication of ITD-and ILD-dependent signals is not required to produce the observed responses. In fact, we showed that a linear-threshold nonlinearity was able to capture the main features of the response. Furthermore, the failure of the linear-threshold model to produce smooth transitions between regions of zero response and positive response may result from the use of mean values in the model. In a more realistic model with trial-to-trial variability, we would expect a linear-threshold model to produce smooth transitions between regions of zero response and positive response. Consistent with the idea of a linear-threshold model for producing nonlinear ICcl responses is the model of Fischer (2005) that treated ICcl as a hidden layer for combining ITD- and ILD-dependent signals. In Fischer (2005), it was shown that a model consisting of additive subthreshold interaction between ITD- and ILD-dependent signals followed by a spiking nonlinearity would lead to multiplicative spiking responses of ICcl neurons. The results of the present study are consistent with the existence of multiplicative spiking responses to ITD- and ILD-dependent signals in ICcl created by either thresholding or pure multiplication because they do not address properties of the subthreshold responses. Intracellular studies are required to determine whether multiplication first emerges in the subthreshold responses of ICcl neurons and thus to differentiate between the multiplicative and linear-threshold models.

A possible mechanism for generating the observed nonlinear spiking responses to ITD and ILD is the presence of GABAergic inhibition at nonpreferred ITD–ILD pairs. GABAergic inhibition is known to shape the responses of ICcl neurons to ITD (Fujita and Konishi 1991; Mori 1997) and ILD (Adolphs 1993). Coupled with a threshold, the presence of GABAergic inhibition at nonpreferred ITD–ILD pairs could limit spiking to discrete regions of ITD and ILD. It has been suggested that *N*-methyl-D-aspartate (NMDA)–mediated responses can serve as a basis for generating multiplicative responses (Koch 1999; Mel 1993). However, NMDA

receptor currents are known to make only a minor contribution to the responses of ICcl neurons (Feldman and Knudsen 1994).

Multiple factors contributed to deviations from multiplication seen in ICcl responses. Interdependence of ITD and ILD was observed in a minority of neurons in the form of changes in preferred values and the shape of the tuning curves when the other variable was changed. The magnitudes of the changes in preferred values of ITD and ILD as a function of the other variable were correlated with the accuracy of the multiplicative model, but not with the difference in accuracy between the additive and multiplicative models. This follows from the fact that both the additive and multiplicative models assume independence of the ITD- and ILD-dependent inputs to ICcl. Therefore when tuning curves change with the other variable, both the multiplicative and additive models fail. Surprisingly, changes in the trough:peak ratio with ILD and changes in the ILD tuning curve flank-height with ITD were only weakly predictive of the accuracy of the multiplicative model or the difference in accuracy between the additive and multiplicative models. One possible explanation for this result is that deviations from the main ITD and ILD tuning curve shapes were mostly observed in areas of low firing rate and thus of minor contribution to model errors. For example, for neurons where the ILD tuning curve changed shape with ITD, the ILD tuning curves were often peaked at preferred ITD values and sigmoidal at nonpreferred ITD values (Fig. 9*B*).

The interdependence of ITD and ILD tunings in this minority of ICcl responses is not consistent with either a linear-threshold or a multiplicative model of the interaction between ITD and ILD tuning. Previous studies suggest that ITD tuning curves of time pathway inputs to ICcl only shift, but do not change shape, with ILD (Viete et al. 1997) and that ILD tuning curves of level pathway inputs to ICcl [from the posterior part of the dorsal lateral lemniscal nucleus (LLDp)] are insensitive to ITD (Egnor 2001; Moiseff and Konishi 1983). The break-down of ITD tuning observed in some neurons at nonsaturating levels (Fig. 1, *C* and *D*) cannot occur in a model where ITD-and ILD-dependent inputs having the properties of NL and LLDp neurons are combined linearly then passed through a static nonlinearity. The inclusion of a multiplication of ITD-and ILD-dependent inputs before a static nonlinearity would similarly fail to produce the observed responses. A more physiologically detailed model of processing in ICcl than either the linear-threshold or multiplicative models may be required to explain the data. Alternatively, similar responses may occur in areas of the auditory pathway before ICcl, but remain unobserved.

## Generating ICx responses

Our results support a model where the operations leading to the emergence of spatially selective auditory neurons in ICx include a nonlinear combination of ITD- and ILD-dependent signals within ICcl neurons that are narrowly tuned to frequency, an additive combination of ICcl responses across frequency, and a population computation that removes deviations from multiplication seen in some ICcl responses. This model is consistent with the basic elements of the standard model for the generation of spatially selective auditory neurons in the owl's midbrain where it is held that ITD and ILD are combined within frequency channels and then converge across frequency to resolve ambiguities in the spatial dependence of ITD and ILD (Arthur 2004; Euston 2000; Euston and Takahashi 2002; Peña and Konishi 2000; Spence et al. 1989). However, the observed responses and the network model presented here together suggest extensions of, and deviations from, previously proposed models.

Our results show that a nonlinearity between ITD and ILD is already present in ICcl. To produce the multiplicative sub-threshold responses to ITD and ILD seen in ICx, a nonlinearity must be present at some point between the site of ITD–ILD convergence in ICcl and the somata of ICx neurons, where intracellular recordings were made. This nonlinearity could arise in various forms, which are not mutually exclusive. One possibility is that the essential nonlinearity

resides in the dendritic trees of ICx neurons (Mel 1993;Peña and Konishi 2001). Nonlinear processing in the dendritic trees of ICx neurons would allow multiplicative responses to arise without the need of a nonlinear combination of ITD and ILD in ICcl. Alternatively, following the model of Fischer (2005), the nonlinearity could arise from the spiking mechanism in ICcl. Our results are consistent with nonlinearity between ITD and ILD arising from the spiking mechanism in ICcl. However, intracellular recording in ICcl is necessary to determine whether multiplicative interaction of ITD and ILD is present in the subthreshold responses of ICcl neurons. Regardless of the mechanism that produces nonlinear interaction between ITD and ILD in ICcl, our model shows that, using a population of ICcl neurons, the nonlinearity present in ICcl is sufficient to produce multiplicative responses in ICx without nonlinear dendritic processing.

The results presented here show that ICcl neurons do not all act as AND gates and thus that the population of ICcl responses must be processed to remove deviations from multiplication that are not seen in ICx. Our network model of ICcl inputs to ICx shows that the nonlinearity observed in ICcl spiking responses to ITD and ILD is sufficient to produce the multiplicative subthreshold responses seen in ICx using a linear combination of ICcl responses. A linear combination of ICcl responses that incorporates all neurons, not just the most multiplicative, over a range of frequencies can reproduce the ICx responses. As noted previously, a population of neurons with a diverse set of tuning curves is sufficient—and possibly beneficial—for accurately computing nonlinear functions of input variables (Eliasmith and Anderson 2003; Shamir and Sompolinsky 2006). Note that although we argue that nonlinear processing in the dendritic trees of ICx neurons is not necessary to produce multiplicative responses, it is an open question whether nonlinear dendritic processing shapes ICx responses to ITD and ILD. There is evidence, however, that auditory responses in ICx include a hyperpolarization at unfavorable ITD–ILD pairs that likely involves postsynaptic inhibition (Peña and Konishi 2001, 2002). Although it is unknown whether this inhibition is spatially tuned, it provides a possible basis for nonlinear processing in ICx neurons that improves the multiplicative interaction of ITD and ILD.

An implication of our model is that the multiplicative model of ICx responses to frequency-independent ITD and ILD proposed by Peña and Konishi (2001) must be refined when considering frequency-dependent ITD and ILD spectra that arise under natural listening conditions. The model proposed here specifies that ITD- and ILD-dependent signals are multiplied only within frequency channels and that ITD- and ILD-dependent signals from nonoverlapping frequency bands are combined linearly in the subthreshold responses of ICx neurons (Fischer 2005; Peña and Konishi 2000). Intuitively, the responses to frequency-independent ITD and ILD of ICx neurons that encode inputs additively across frequency can appear multiplicative if the responses to different frequency components have similar shapes. This is especially true for neurons with receptive fields near the center of gaze where the associated ITD and ILD spectra are roughly flat (Keller et al. 1998). It remains to be seen whether responses to frequency-independent ITD and ILD of ICx neurons with highly frequency dependent preferred ITD and ILD spectra, and therefore peripherally located best locations, are well described by a multiplicative model. Future tests are also necessary to evaluate the claim that ITD- and ILD-dependent inputs of different frequencies will interact linearly at the subthreshold level in ICx. The restriction of multiplication to individual frequency channels may be important for the representation of multiple concurrent sound sources with nonoverlapping frequency spectra in the auditory space map (Keller and Takahashi 2005; Takahashi and Keller 1994).

In conclusion, we find that ICcl is the site in the barn owl's midbrain sound localization pathway where multiplicative selectivity for ITD- and ILD-dependent signals arises. Deviations from multiplication are observed in ICcl that are not present in ICx, indicating that processing must

occur between ICcl and ICx to remove the deviations. We hypothesize that a linear combination of ICcl neurons across frequency is sufficient to produce the multiplicative tuning to ITD- and ILD-dependent signals seen in ICx.

## ACKNOWLEDGMENTS

We thank K. Mori and R. Wessel for providing comments on earlier versions of the manuscript, B. Christianson for discussions about data analysis, and G. Akutagawa for histology.

GRANTS

This work was supported by National Institute on Deafness and Other Communication Disorders Grants DC-00134 to M. Konishi and DC-007690 to J. L. Peña.

## REFERENCES

Adolphs R. Bilateral inhibition generates neural responses tuned to interaural level differences in the auditory brainstem of the barn owl. J Neurosci 1993;13:3646–3668.

Andersen RA, Snyder LH, Bradley DC, Xing J. Multimodal representation of space in the posterior parietal cortex and its use in planning movements. Annu Rev Neurosci 1997;20:303–330. [PubMed: 9056716]

Arthur BJ. Sensitivity to spectral interaural intensity difference cues in space-specific neurons of the barn owl. J Comp Physiol A Sens Neural Behav Physiol 2004;190:91–104.

Brainard MS, Knudsen EI. Experience-dependent plasticity in the inferior colliculus: a site for visual calibration of the neural representation of auditory space in the barn owl. J Neurosci 1993;13:4589–4608. [PubMed: 8229186]

Egelhaaf M, Borst A, Reichardt W. Computational structure of a biological motion-detection system as revealed by local detector analysis in the fly's nervous system. J Opt Soc Am 1989;6:1070–1087.

Egnor SER. Effects of binaural decorrelation on neural and behavioral processing of interaural level differences in the barn owl (*Tyto alba*). J Comp Physiol A Sens Neural Behav Physiol 2001;187:589–595.

Eliasmith, C.; Anderson, CH. Neural Engineering. Cambridge, MA: MIT Press; 2003.

Euston, DR. From Spectrum to Space: The Integration of Frequency-Specific Intensity Cues to Produce Auditory Spatial Receptive Fields in the Barn Owl Inferior Colliculus (PhD dissertation). Eugene, OR: Univ. of Oregon; 2000. http://hdl.handle.net/1794/143 Online

Euston DR, Takahashi TT. From spectrum to space: the contribution of level difference cues to spatial receptive fields in the barn owl inferior colliculus. J Neurosci 2002;22:284–293. [PubMed: 11756512]

Feldman DE, Knudsen EI. NMDA and non-NMDA glutamate receptors in auditory transmission in the barn owl inferior colliculus. J Neurosci 1994;14:5939–5958. [PubMed: 7931555]

Fischer, BJ. A Model of the Computations Leading to a Representation of Auditory Space in the Midbrain of the Barn Owl (DSc dissertation). St. Louis, MO: Washington Univ; 2005. online http://www.its.caltech.edu/~fischerb Online

Fujita I, Konishi M. The role of GABAergic inhibition in processing of interaural time difference in the owl's auditory system. J Neurosci 1991;11:722–739. [PubMed: 2002359]

Gabbiani F, Krapp HG, Koch C, Laurent G. Multiplicative computation in a visual neuron sensitive to looming. Nature 2002;420:320–324. [PubMed: 12447440]

Keller CH, Hartung K, Takahashi TT. Head-related transfer functions of the barn owl: measurement and neural responses. Hear Res 1998;118:13–34. [PubMed: 9606058]

Keller CH, Takahashi TT. Localization and identification of concurrent sounds in the owl's auditory space map. J Neurosci 2005;25:10446–10461. [PubMed: 16280583]

Knudsen EI. Subdivisions of the inferior colliculus in the barn owl (*Tyto alba*). J Comp Neurol 1983;218:174–186. [PubMed: 6886070]

Knudsen EI, Konishi M. A neural map of auditory space in the owl. Science 1978a;200:795–797. [PubMed: 644324]

Knudsen EI, Konishi M. Space and frequency are represented separately in auditory midbrain of the owl. J Neurophysiol 1978b;41:870–884. [PubMed: 681991]

Koch, C. Biophysics of Computation: Information Processing in Single Neurons. New York: Oxford Univ. Press; 1999.

Koch, C.; Poggio, T. Single Neuron Computation. Cambridge, MA: Academic Press; 1992. Multiplying with synapses and neurons.

Mazer, JA. Integration of Parallel Processing Streams in the Inferior Colliculus of the Barn Owl (PhD dissertation). Pasadena, CA: California Institute of Technology; 1995.

Mel BW. The sigma-pi model neuron: roles of the dendritic tree in associative learning. Soc Neurosci Abstr 1990;16:205.4.

Mel BW. Synaptic integration in an excitable dendritic tree. J Neurophysiol 1993;70:1086–1101. [PubMed: 8229160]

Moiseff A, Konishi M. Neuronal and behavioral sensitivity to binaural time differences in the owl. J Neurosci 1981;1:40–48. [PubMed: 7346557]

Moiseff A, Konishi M. Binaural characteristics of units in the owl's brainstem auditory pathway: precursors of restricted spatial receptive fields. J Neurosci 1983;3:2553–2562. [PubMed: 6655499]

Mori K. Across-frequency nonlinear inhibition by GABA in processing of interaural time difference. Hear Res 1997;111:22–30. [PubMed: 9307308]

Olsen JF, Knudsen EI, Esterly SD. Neural maps of interaural time and intensity differences in the optic tectum of the barn owl. J Neurosci 1989;9:2591–2605. [PubMed: 2746340]

Peña JL, Konishi M. Cellular mechanisms for resolving phase ambiguity in the owl's inferior colliculus. Proc Natl Acad Sci USA 2000;97:11787–11792. [PubMed: 11050210]

Peña JL, Konishi M. Auditory spatial receptive fields created by multiplication. Science 2001;292:249–252. [PubMed: 11303092]

Peña JL, Konishi M. From postsynaptic potentials to spikes in the genesis of auditory spatial receptive fields. J Neurosci 2002;22:5652–5658. [PubMed: 12097516]

Poggio T. A theory of how the brain might work. Cold Spring Harbor Symp Quant Biol 1990;55:899–910. [PubMed: 2132866]

Pouget A, Dayan P, Zemel R. Inference and computation with population codes. Annu Rev Neurosci 2003;26:381–410. [PubMed: 12704222]

Pouget A, Sejnowski TJ. Spatial transformations in the parietal cortex using basis functions. J Cog Neurosci 1997;9:222–237.

Salinas E, Abbott LF. Invariant visual responses from attentional gain fields. J Neurophysiol 1997;77:3267–3272. [PubMed: 9212273]

Shamir M, Sompolinsky H. Implications of neuronal diversity on population coding. Neural Comput 2006;18:1951–1986. [PubMed: 16771659]

Spence, CD.; Pearson, JC.; Gelfand, JJ.; Peterson, RM.; Sullivan, WE. Neuronal maps for sensory-motor control in the barn owl. In: Touretzky, D., editor. Advances in Neural Information Processing Systems. vol. 1. Cambridge, MA: MIT Press; 1989.

Stern RM, Colburn HS. Theory of binaural interaction based on auditorynerve data. IV. A model for subjective lateral position. J Acoust Soc Am 1978;64:127–140. [PubMed: 711991]

Sullivan WE, Konishi M. Segregation of stimulus phase and intensity coding in the cochlear nucleus of the barn owl. J Neurosci 1984;4:1787–1799. [PubMed: 6737041]

Sun HJ, Frost BJ. Computation of different optical variables of looming objects in pigeon nucleus rotundus neurons. Nat Neurosci 1998;1:296–303. [PubMed: 10195163]

Takahashi TT, Keller CH. Representation of multiple sources in the owl's auditory space map. J Neurosci 1994;14:4780–4793. [PubMed: 8046449]

Takahashi TT, Konishi M. The projections of the cochlear nuclei and nucleus laminaris to the inferior colliculus of the barn owl. J Comp Neurol 1988;274:190–211. [PubMed: 2463286]

Takahashi TT, Moiseff A, Konishi M. Time and intensity cues are processed independently in the auditory system of the owl. J Neurosci 1984;4:1781–1786. [PubMed: 6737040]

Takahashi TT, Wagner H, Konishi M. The role of the commissural projections in the representation of bilateral space in the barn owl's inferior colliculus. J Comp Neurol 1988;281:545–554. [PubMed: 2708580]

Viete S, Peña JL, Konishi M. Effects of interaural intensity difference on the processing of interaural time differences in the owl's nucleus laminaris. J Neurosci 1997;17:1815–1824. [PubMed: 9030640]

Wagner H, Takahashi TT, Konishi M. Representation of interaural time difference in the central nucleus of the barn owl's inferior colliculus. J Neurosci 1987;7:3105–3116. [PubMed: 3668618]

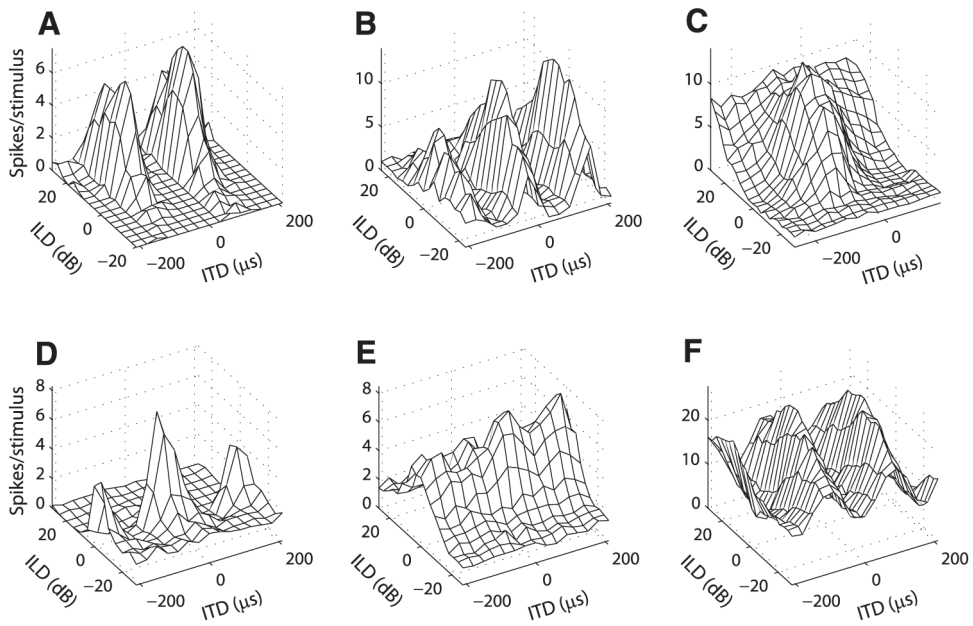


**FIG. 1.**

Example responses to interaural time difference (ITD) and interaural level difference (ILD) pairs in lateral shell of the central nucleus of the inferior colliculus (ICcl) neurons. Examples are representative of the different types of responses observed in the sample as discussed in RESULTS.

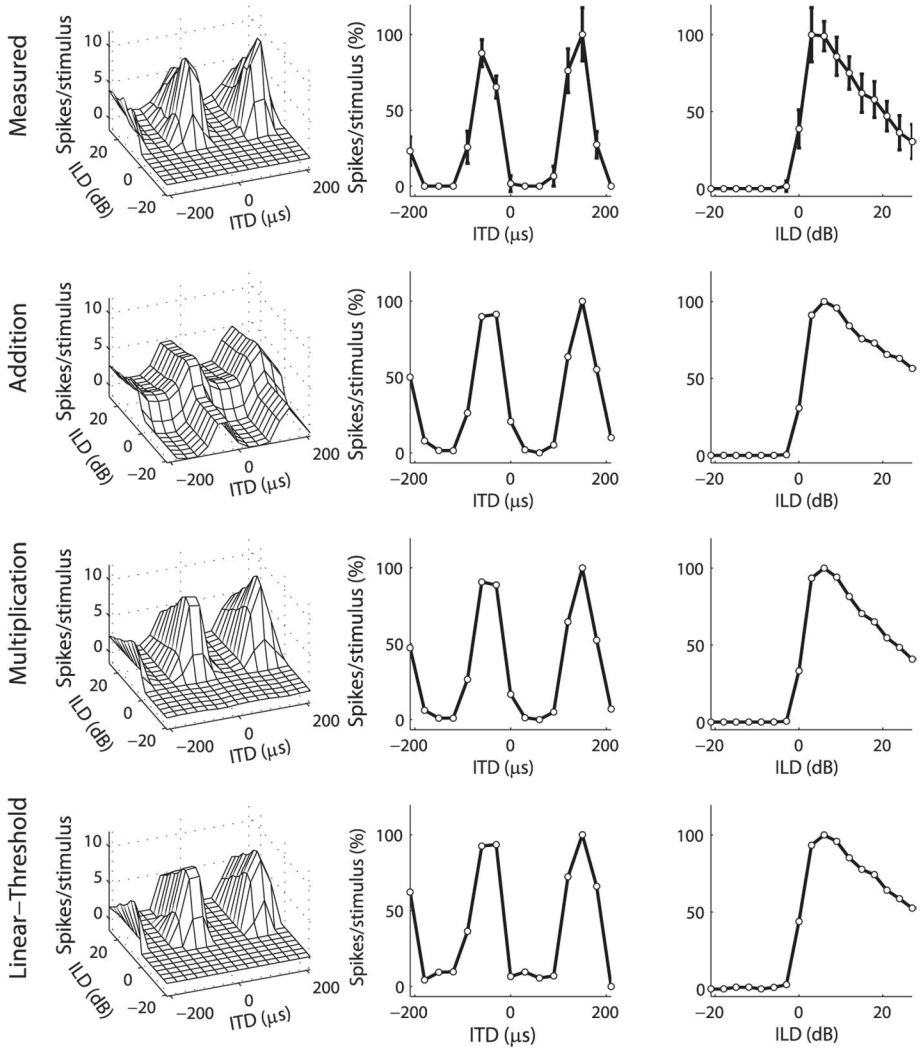


**FIG. 2.**

Example ICcl neuron where the multiplicative model fit the data better than did the additive model. *Top row*: ITD–ILD response matrix of an ICcl neuron (*left column*) along with its ITD and ILD tuning curves (*center* and *right columns*, respectively). Error bars represent the SD. Approximations to the data (*left column*) were formed by combining a function of ITD (*center column*) with a function of ILD (*right column*) either additively (*2nd row*), multiplicatively (*3rd row*), or using addition and a threshold (*bottom row*). ITD and ILD tuning curves of the data, as well as ITD and ILD model components, are plotted as the percentage of response height. Normalized root-mean-square (RMS) errors for the additive, multiplicative, and linear-threshold models were 13.95, 5.56, and 6.70%, respectively.

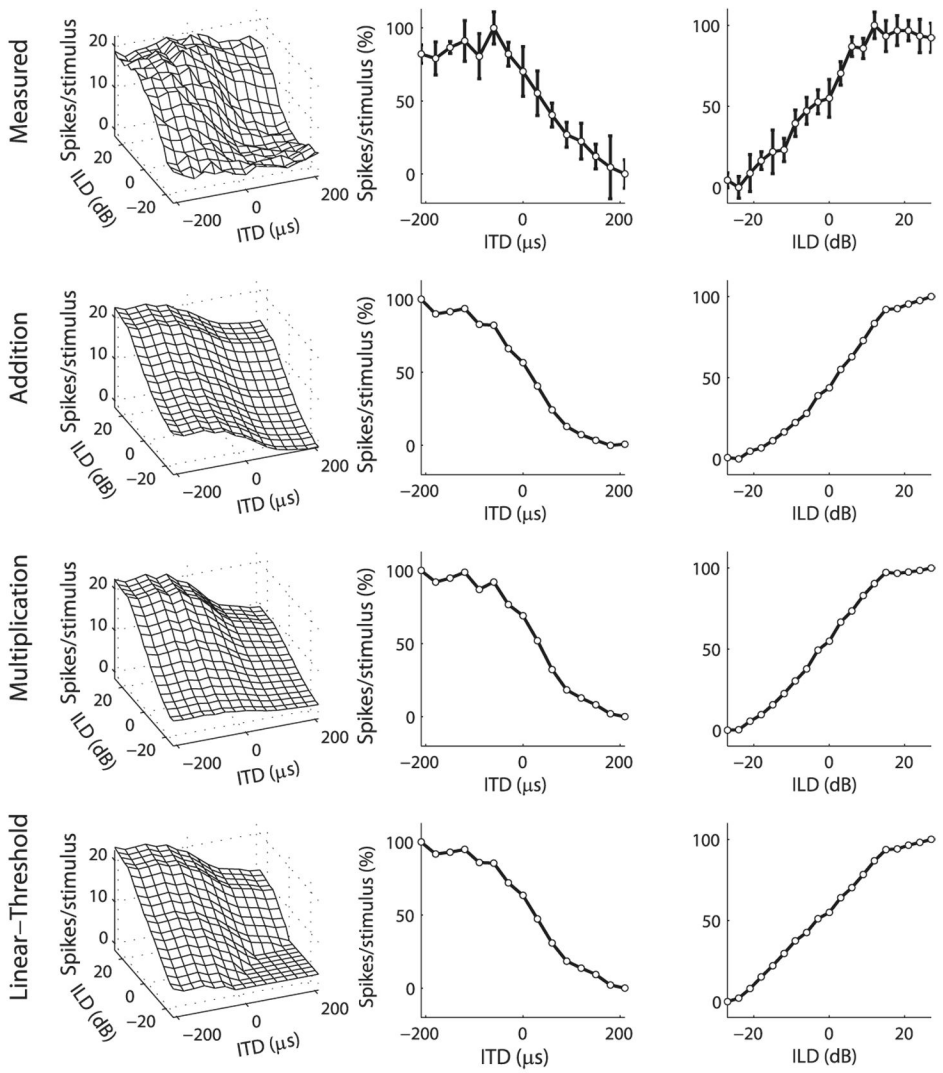


**FIG. 3.**

Example ICcl neuron where the additive model fit the data better than did the multiplicative model. Plots are as in Fig. 2. Normalized RMS errors for the additive, multiplicative, and linear-threshold models were 11.19, 12.96, and 9.19%, respectively.

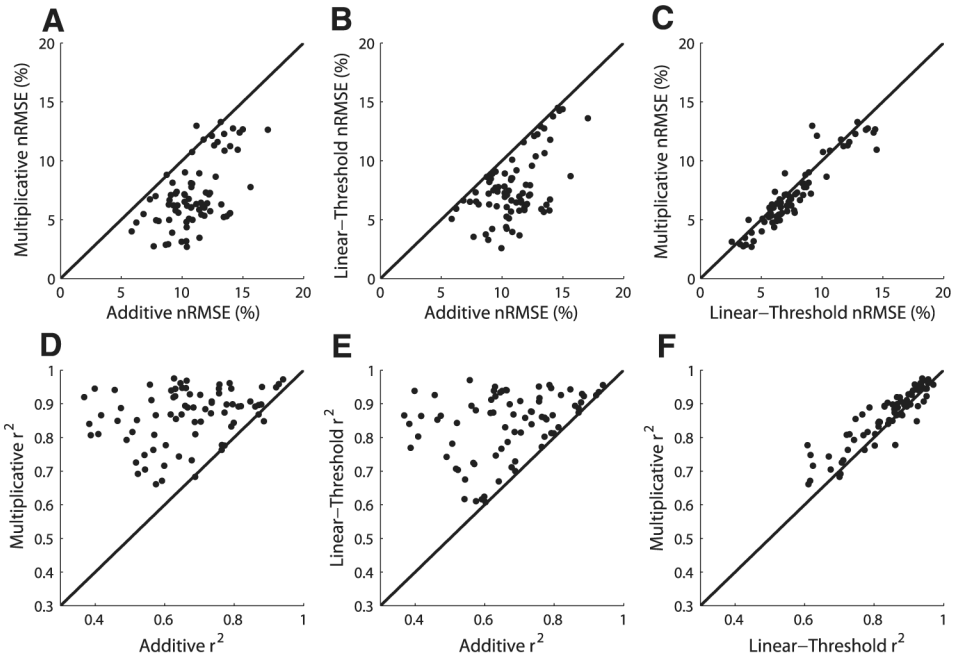


**FIG. 4.**

*A–C*: comparison of the normalized RMS errors in additive, multiplicative, and linear-threshold models of the ITD–ILD response matrix. *D–F*: comparison of the correlation between the data and the model approximation in additive, multiplicative, and linear-threshold models of the ITD–ILD response matrix.

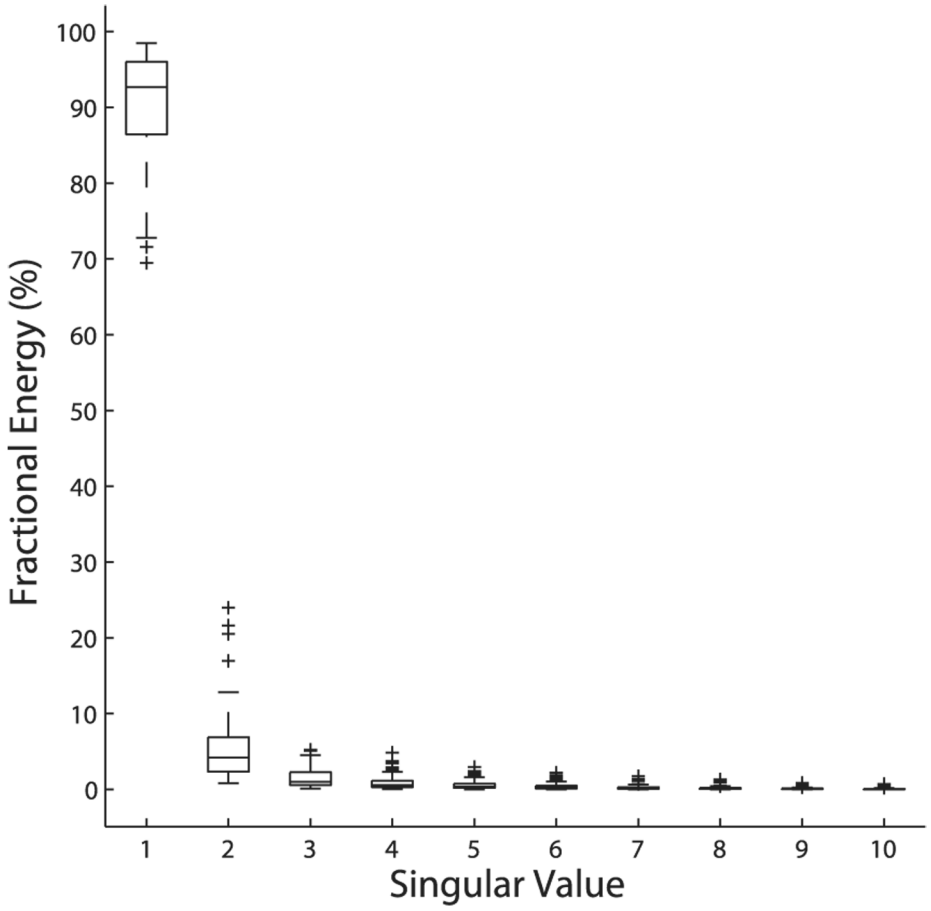


**FIG. 5.**

Fractional energy in the first 10 singular values of the singular value decomposition of the ITD–ILD response matrix in ICcl. Boxes extend from the first quartile to the third quartile of the sample, with the center line marking the median. Outliers (+) are data points >1.5 times the interquartile range of the sample. A mean of 90.37 ± 7.21% of the energy was in the first singular value ($n$ = 77; median 92.67%, first quartile 86.44%, third quartile 96.03%).

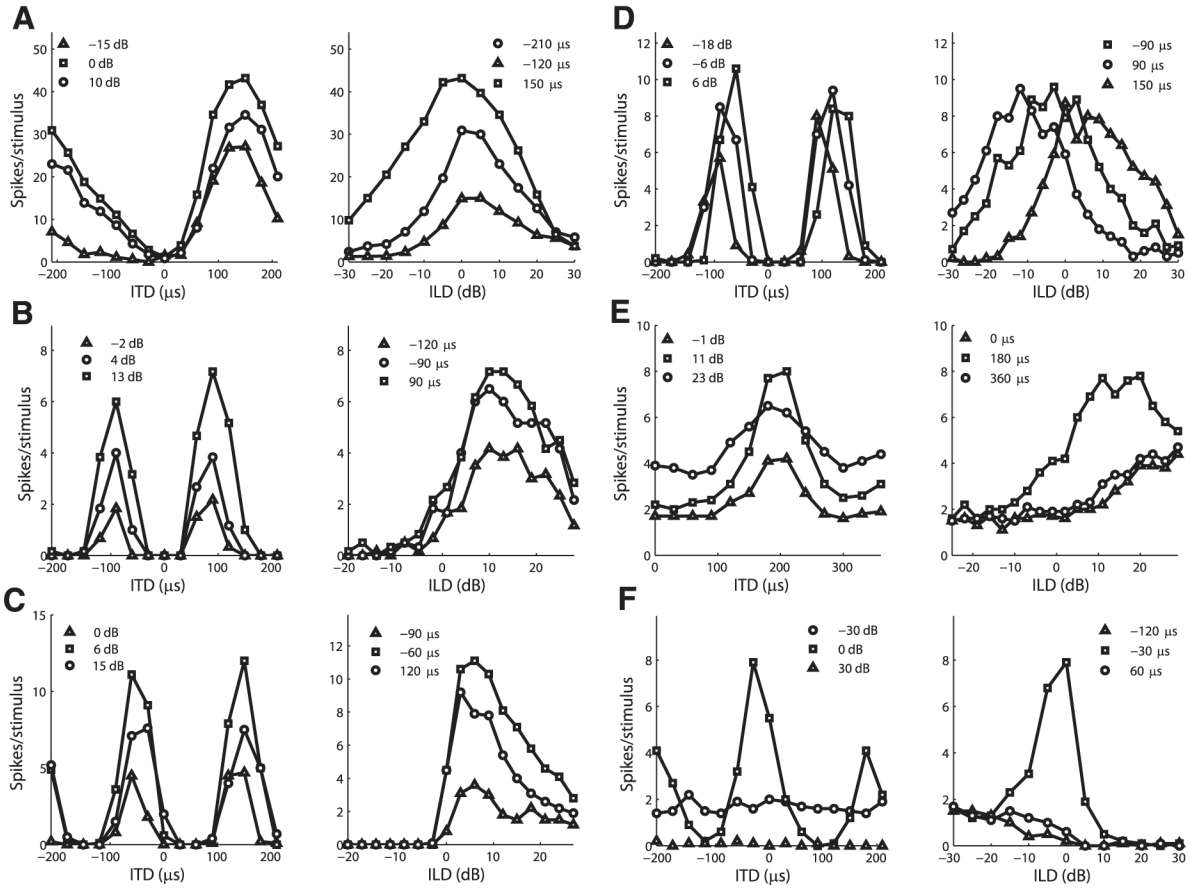


**FIG. 6.**

*A–C*: example neurons that qualitatively agree with the multiplicative model. *Left column*: ITD tuning curves at different ILDs. *Right column*: ILD tuning curves at different ITDs. Pairs in each row are for the same neuron. *D–F*: example neurons that show deviations from the multiplicative model. Example neurons show tuning curves that shift with the other variable (*D*), ITD tuning curves that differ by a constant bias (*E*), and ILD tuning curves that are peaked only for preferred ITD values (*F*).

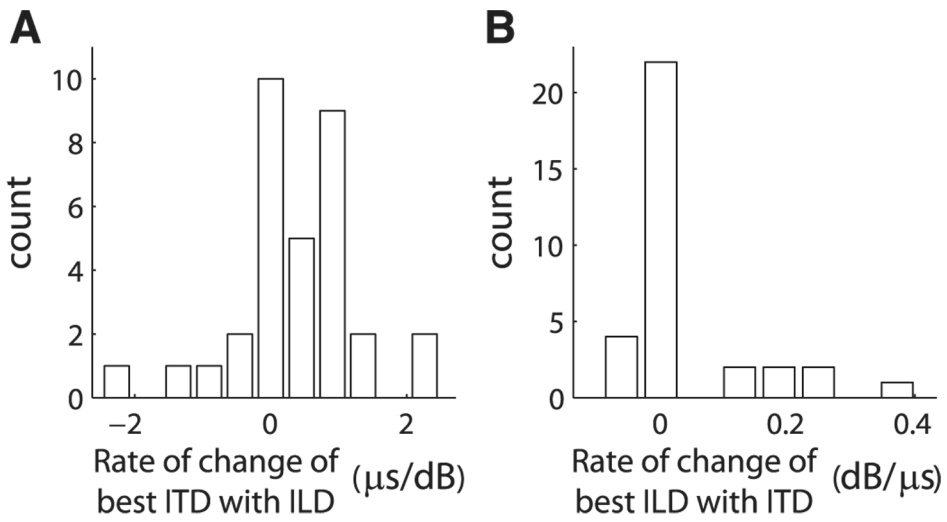


**FIG. 7.**

*A*: rate of change of best ITD with ILD. Rate of change is defined for neurons where there were at least 5 significant ITD tuning curves and the RMS error in the best linear fit to the change in best ITD with ILD was ≤30 μs (33/77; see METHODS). *B*: rate of change of best ILD with ITD. Rate of change is defined for neurons where there were at least 5 significant ILD tuning curves and the RMS error in the best linear fit to the change in best ILD with ITD was ≤6 dB (33/77; see METHODS).

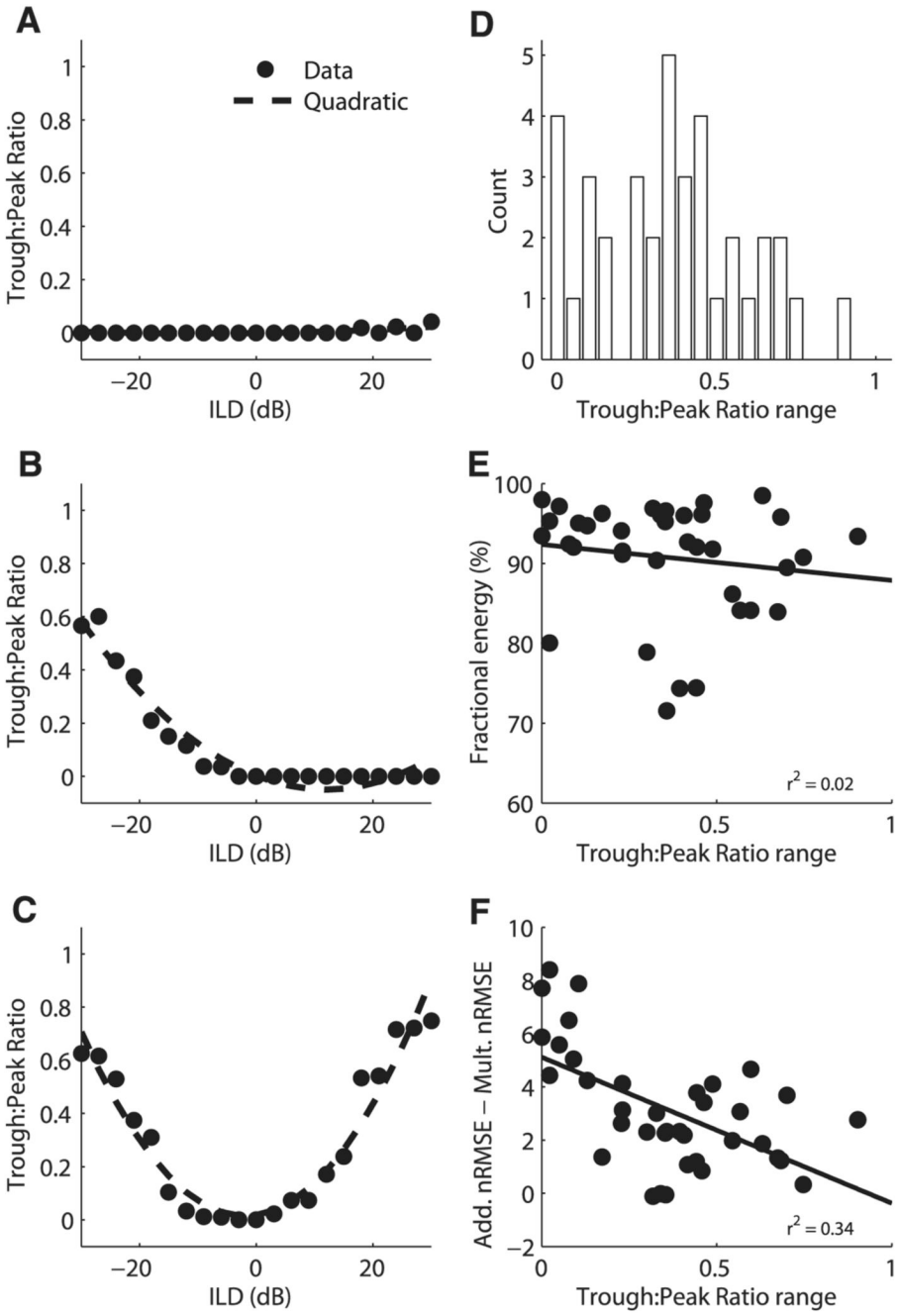


**FIG. 8.**

Trough:peak ratio of ITD tuning curves as a function of ILD. Trough:peak ratio for example neurons showing little variation with ILD (*A*), an increase at one end of the ILD range (*B*), and increases at both ends of the ILD range (*C*). Data are plotted along with the least-squares quadratic fit. Average RMS error in the quadratic fit over 37 neurons with at least 5 significant ITD tuning curves was 0.049 ± 0.043. *D*: difference between the maximum and minimum trough:peak ratios at different ILDs in individual neurons ($n = 37$). *E* and *F*: difference between the maximum and minimum trough:peak ratios at different ILDs plotted against the fractional energy in the first singular value of the singular value decomposition of the ITD–ILD response

matrix (*E*) and the difference between the additive and multiplicative nRMS errors in the approximation to the ITD–ILD response matrix (*F*).

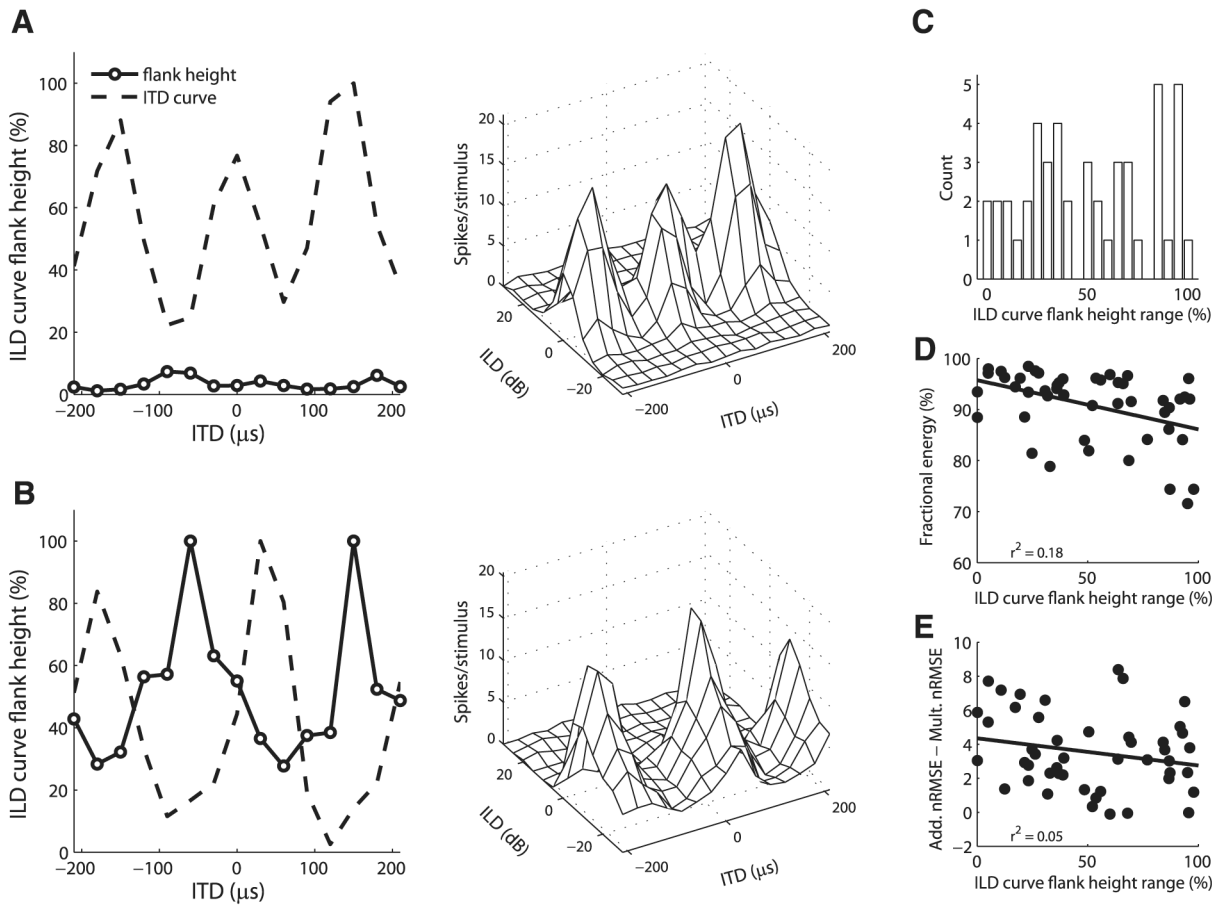


**FIG. 9.**

ILD tuning curve flank-height as a function of ITD. *A*: example neuron where the ILD tuning curve flank-height varied little with ITD. ITD–ILD response matrix (*right*) shows that the neuron had peaked ILD tuning for each ITD value. *B*: example neuron where the ILD tuning curve flank-height varied with ITD. Height of the ILD tuning curve flank was smallest for ITD values corresponding to peaks in the ITD curve. ITD–ILD response matrix (*right*) shows that the neuron had sigmoidal ILD tuning for nonpreferred ITD values and open-peaked ILD tuning for preferred ITD values. *C*: difference between the maximum and minimum ILD tuning curve flank-heights at different ITDs in individual neurons ($n = 47$). *D* and *E*: difference between the maximum and minimum ILD tuning curve flank-heights at different ITDs plotted against the fractional energy in the first singular value of the singular value decomposition of the ITD–ILD response matrix (*D*) and the difference between the additive and multiplicative nRMS errors in the approximation to the ITD–ILD response matrix (*E*).

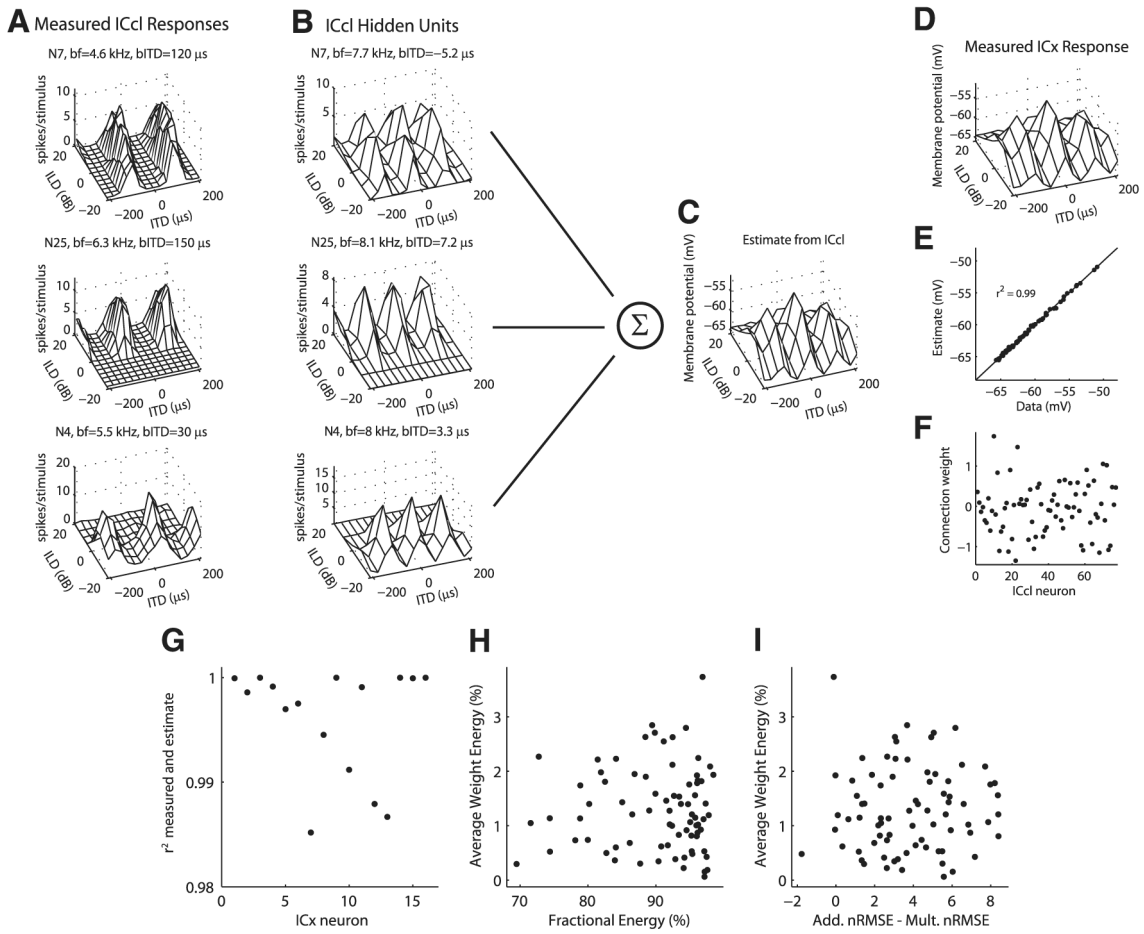


**FIG. 10.**

Estimate of the subthreshold response of external nucleus of the inferior colliculus (ICx) neurons from the spiking responses of ICcl neurons. *A*: examples of measured spiking responses of ICcl neurons to ITD and ILD. For each neuron, the best frequency (bf) and best ITD (bITD) are displayed, for comparison with the corresponding hidden layer units in *B*. *B*: hidden layer units corresponding to the neurons in *A* derived from a parametric fit to the measured response (see METHODS). Best frequency and best ITD of the hidden unit were modified to be consistent with the ICx unit in *D*, but the dependence of ITD tuning on ILD is the same as in the measured response. *C*: estimate of the ICx response in *D* from a linear combination of ICcl hidden unit responses using the weights plotted in *F*. *E*: correlation between the model estimate shown in *C* and the measured ICx data shown in *D*. *G*: squared correlation coefficients of the model estimate and the measured ICx data for 16 ICx neurons. ICx data are from Peña and Konishi (2001). *H* and *I*: energy in each ICcl unit's connection weight $(\omega_i^2 / \sum_n \omega_n^2) \times 100\%$, averaged over 16 ICx neurons plotted against the fractional energy in the first singular value of the singular value decomposition of the ITD–ILD response matrix (*H*) and the difference between the additive and multiplicative normalized RMS errors in the approximation to the ITD–ILD response matrix (*I*).